

## Role of the N-related localized states in the electron emission properties of a GaAsN quantum well

Meng-Chien Hsieh, Jia-Feng Wang, Yu-Shou Wang, Cheng-Hong Yang, Ross C. C. Chen, Chen-Hao Chiang, Yung-Fu Chen, and Jenn-Fang Chen

Citation: *Journal of Applied Physics* **110**, 103709 (2011); doi: 10.1063/1.3663436

View online: <http://dx.doi.org/10.1063/1.3663436>

View Table of Contents: <http://scitation.aip.org/content/aip/journal/jap/110/10?ver=pdfcov>

Published by the [AIP Publishing](#)

---

### Articles you may be interested in

[Optimum indium composition for \(Ga, In\)\(N, As\) GaAs quantum wells emitting beyond 1.5  \$\mu\$ m](#)  
*Appl. Phys. Lett.* **88**, 091111 (2006); 10.1063/1.2180441

[Characteristic of rapid thermal annealing on GaIn\(N\)\(Sb\)As GaAs quantum well grown by molecular-beam epitaxy](#)  
*J. Appl. Phys.* **99**, 034903 (2006); 10.1063/1.2164539

[Thermally induced diffusion in GaInNAs GaAs and GaInAs GaAs quantum wells grown by solid source molecular beam epitaxy](#)  
*J. Appl. Phys.* **97**, 013506 (2005); 10.1063/1.1825632

[Role of N ions in the optical and morphological properties of InGaAsN quantum wells for 1.3 – 1.5  \$\mu\$ m applications](#)  
*Appl. Phys. Lett.* **85**, 1940 (2004); 10.1063/1.1790591

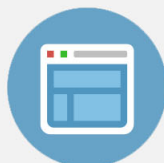
[Electron traps in Ga\(As,N\) layers grown by molecular-beam epitaxy](#)  
*Appl. Phys. Lett.* **80**, 2120 (2002); 10.1063/1.1463214

---



## Re-register for Table of Content Alerts

Create a profile.



Sign up today!



# Role of the N-related localized states in the electron emission properties of a GaAsN quantum well

Meng-Chien Hsieh,<sup>a)</sup> Jia-Feng Wang, Yu-Shou Wang, Cheng-Hong Yang, Ross C. C. Chen, Chen-Hao Chiang, Yung-Fu Chen, and Jenn-Fang Chen

*Department of Electrophysics, National Chiao Tung University, Hsinchu, Taiwan 30050, Republic of China*

(Received 29 June 2011; accepted 24 October 2011; published online 23 November 2011)

This study elucidates the influence of the N-related localized states on electron emission properties of a GaAsN quantum well (QW) that is grown by molecular beam epitaxy. The N-related localized states in a GaAsN QW are identified as both optical and electrical electron trap states. Furthermore, exactly how N-related localized states influence the electron emission properties of a GaAsN quantum well is examined. The presence of N-related localized states effectively suppresses the tunneling emission of GaAsN QW electron states, leading to a long electron emission time for the GaAsN QW electron states. Thermal annealing can reduce the number of N-related localized states, resulting in a recovery of the tunneling emission for GaAsN QW electron states. Increasing the annealing temperature can restore the electron emission behavior of GaAsN QW to the typical electron tunneling emission for a high-quality QW. © 2011 American Institute of Physics. [doi:10.1063/1.3663436]

## I. INTRODUCTION

III–V alloys containing nitrogen (commonly referred to as dilute nitrides), such as  $\text{GaAs}_{1-x}\text{N}_x$  and  $\text{In}_y\text{Ga}_{1-y}\text{As}_{1-x}\text{N}_x$ , have received considerable attention experimentally and theoretically in the recent decade. They are characterized by a large decrease of the band gap upon incorporation of a small amount of nitrogen. III–V alloys are thus promising materials for applications such as vertical cavity surface-emitting lasers that are operated in the coveted 1.3–1.5  $\mu\text{m}$  range<sup>1,2</sup> and high efficiency multijunction solar cells.<sup>3</sup> However, nitrogen atoms result in a carrier localization effect at low temperatures, often making photoluminescence (PL) weaker than in a N-free system.<sup>4</sup> As is well known, the optical quality of dilute nitrides can be improved using rapid thermal annealing (RTA). However, even for annealed materials, low-temperature PL spectra obtained at low excitation conditions are dominated by the recombination of localized carriers (excitons) that are trapped at local potential minima (N-related localized states).<sup>5,6</sup> Nevertheless, the exact nature of N-related localized states is still controversial. Hence, understanding the N-related localized states in GaAsN bulk and quantum wells (QWs) is particularly worthwhile, from both physics and device design perspectives. Recent first-principle calculations account for the different possible local environments of incorporated N atoms (single-atom impurities, pairs, or other clusters) and predict (1) the formation of N cluster states (CSs) that give rise to deep states in the gap; (2) the perturbation of host states (PHSs = perturbed host states), and (3) the formation of the band structure of the alloy owing to the interaction between CSs and PHSs.<sup>7,8</sup> According to these calculations, these clusters of N atoms generate states along the edge of the conduction band (CB), resulting in the formation of a fluctuation potential that is responsible for N-related localized states. Despite these achievements, to our knowledge, the influence of

the N-related localized states in GaAsN QW has not been investigated in detail in terms of their electron emission properties.

This study investigates the role of the N-related localized states in the electron emission properties of a GaAsN quantum well by PL, admittance spectroscopy, and deep-level transient spectroscopy (DLTS) combined with RTA. The N-related localized states are first identified by PL measurements, and the DLTS measurement also confirms the PL measurement results. Detailed electron emission properties of the GaAsN QW electron states are obtained from the temperature-dependent capacitance-frequency (C-F) spectra. Furthermore, exactly how N-related localized states influence the electron emission properties of a GaAsN quantum well is examined based on experimental results and a theoretical model.

## II. EXPERIMENTS

GaAsN/GaAs single quantum well (SQW) samples were grown on  $n^+$ -GaAs (001) substrates by molecular beam epitaxy (MBE). An EPI-Unibulb radio frequency (rf) plasma source was used to provide nitrogen species from a pure  $\text{N}_2$  gas. The gallium was supplied from conventional Knudsen effusion cells; As in the form of  $\text{As}_2$  was supplied from a cracker source. The growth was started with a 0.3  $\mu\text{m}$  Si-doped GaAs layer of  $4 \times 10^{16} \text{cm}^{-3}$  grown at 580 °C, followed by a 80 Å-thick GaAsN layer, grown at 480 °C. To avoid the introduction of any unwanted shallow impurity states, the GaAsN layer was undoped. After the growth of the GaAsN layer, the growth temperature was increased to 580 °C for the growth of a 0.3  $\mu\text{m}$  Si-doped GaAs top layer of  $4 \times 10^{16} \text{cm}^{-3}$ . The N composition was estimated by the PL peak energy to be about 2.7%. The InGaAsN/GaAs SQW samples were also grown on  $n^+$ -GaAs (001) substrates by MBE. A 0.3  $\mu\text{m}$  Si-doped GaAs layer of  $\sim 6 \times 10^{16} \text{cm}^{-3}$  was first grown at 580 °C, followed by a 60 Å-thick

<sup>a)</sup>Electronic mail: markvipmail@yahoo.com.tw.

InGaAsN layer containing 2% N and grown at 420 °C. After the growth of the InGaAsN layer, a 0.3  $\mu\text{m}$  Si-doped GaAs layer of  $\sim 6 \times 10^{16} \text{ cm}^{-3}$  was grown at 580 °C to terminate the whole structure. The In and Ga cell temperatures were controlled to yield a composition of 34% In and 66% Ga. X-ray diffraction patterns and their simulation were used to determine the In and N compositions by first determining the In composition from an InGaAs/GaAs SQW structure and then determining the N composition, assuming the In composition was the same. The InGaAsN thickness in the 4.4 A/s (normal growth rate (NGR)) and 2.8 A/s (low growth rate (LGR)) samples was checked using the interference fringes of the x-ray (400) diffraction patterns. The growth rates of the InGaAsN layer were varied by scaling the In and Ga fluxes to grow to the same thickness. Schottky contact was established by evaporating Al on the samples with a dot diameter of 800  $\mu\text{m}$ . Next, PL spectra were obtained by a frequency doubled YAG:Nd laser ( $\lambda = 532 \text{ nm}$ ) and an InGaAs detector. Finally, admittance spectroscopy was performed using a HP 4194 A impedance analyzer.

### III. RESULTS AND DISCUSSION

Figure 1(a) shows the power-dependent PL spectra (at 30 K) of the 80 A as-grown sample. In this figure, two broad emission peaks appear at 1.16 eV and 1.03 eV. Comparing these results with the annealing results (as discussed later) reveals that the broad emission peak appearing at the high-energy side (1.16 eV) is GaAsN QW emission peak. A previous study identified the broad emission peak at 1.03 eV as associated with emission between the GaAsN QW electron states and a deep defect level at about 190 meV above the GaAs valence band.<sup>9</sup> This study also evaluates the N content in GaAsN QW by using the emission energy of the GaAsN QW combined with band anticrossing model and 1-D quantum well simulation.<sup>4,10–12</sup> Therefore, the N content in GaAsN QW is estimated to be  $N = 2.7\%$ . This N content is also similar to a previous observation,<sup>13</sup> which has a sample structure and emission energy similar to those in our investigated samples. Figs. 1(b) and 1(c) show the power-dependent PL spectra (at 30 K) of the 80 A sample after RTA at (b) 700 °C and (c) 800 °C for 3 min. According to Figs. 1(a)–1(c), RTA splits the broad as-grown GaAsN QW emission into two peaks, a low energy peak at around 1.15~1.17 eV and a high energy peak at around 1.17~1.20 eV. Additionally, thermal annealing increases the PL intensity of the GaAsN QW emission and reduces the PL linewidth of the GaAsN QW emission. As is well known, post-growth thermal annealing<sup>14–17</sup> significantly improves the quality of the alloy. Moreover, according to previous studies,<sup>14,15</sup> annealing of the bulk GaAsN layers increases photoluminescence (PL) intensity and reduces PL linewidth. Thus, the broad emission peak appearing at the high-energy side (1.16 eV) in as-grown sample is identified as GaAsN QW emission peak. Also, the high energy peak in RTA samples is also identified as GaAsN QW emission peak. Furthermore, the low energy peak exhibits a limited-filling feature relative to GaAsN QW emission peak. According to the limited-filling feature and the relative emission peak position, this low energy emission is the typical emission from

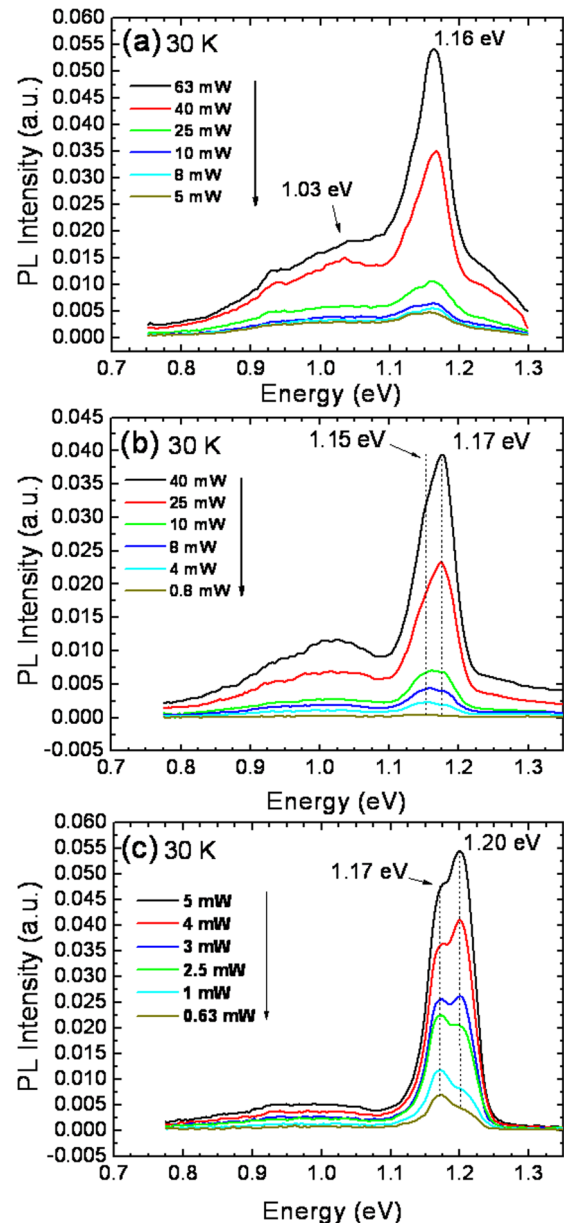


FIG. 1. (Color online) 30 K power-dependent PL spectra of the 80 A (a) as-grown, (b) RTA 700 °C for 3 min, and (c) RTA 800 °C for 3 min samples.

N-related localized states.<sup>5,18–20</sup> At a low excitation power, only the low energy emission is observed, since most free carriers are in the N-related localized states. Notably, increasing the excitation power increases the relative intensity of the high energy (delocalized GaAsN QW states) emission because of carrier saturation in the N-related localized states. At high excitation, the GaAsN QW emission with a narrow linewidth dominates the PL spectra. Besides, the high N concentration ( $N = 2.7\%$ ) in our investigated samples causes severe N-composition fluctuation, subsequently leading to the GaAsN layer having more different forms of N-atoms clusters. Additionally, severe N-composition fluctuation increases the PL linewidth of the GaAsN QW emission; more different forms of N-atoms clusters generate more N-related localized states along the CB edge,<sup>7,8</sup> leading to the broad linewidth of the emissions of the N-related localized states. Thus,

combining the broad GaAsN QW PL linewidth and the broad PL linewidth of the N-related localized states results in a broad emission peak of GaAsN QW at the high-energy side (1.16 eV) in our as-grown sample.

Next, exactly how the N-related localized states influence electron emission properties of a GaAsN quantum well is examined. Figure 2 shows the temperature-dependent C-V depth profiles and the corresponding C-V spectra (as shown on the right side) of the 80 Å (a) as-grown, (b) RTA 700 °C, and (c) RTA 800 °C samples. In the as-grown sample, the concentration peak appearing at 0.344  $\mu\text{m}$  is close to the growth position of the GaAsN QW ( $\sim 0.3 \mu\text{m}$ ). Additionally, at low temperatures, the electron emission from this state cannot follow the ac signal, thus exhibiting a long electron emission time constant. Moreover, increasing the annealing temperature restores the electron emission time of this peak to a short time constant, which exhibits a typical electron emission property of a high-quality QW. Thus, the concentration peak appearing at 0.344  $\mu\text{m}$  is identified as the GaAsN QW electron states signal. Detailed emission times ( $\tau$ ) of the GaAsN QW electron states are obtained from the temperature-dependent capacitance-frequency (C-F) spectra, as shown in Fig. 3. The temperature-dependent C-F spectra are measured at (a)  $-2.3 \text{ V}$  for as-grown sample and (b)

$-2.25 \text{ V}$  for RTA 700 °C sample, which corresponds to the frequency dispersion of the GaAsN QW electron states signal. A capacitance drop from a high plateau to a low plateau is visible as frequency is increased, which is due to the inability of the electrons to follow an ac modulating signal. The emission times are obtained from the inverse of the inflexion frequencies at which the capacitance drops. Figure 4 shows the obtained Arrhenius plots of the emission times from (a)  $-1.5$  to  $-4.4 \text{ V}$  for as-grown sample and (b)  $-1.5 \text{ V}$  to  $-4 \text{ V}$  for RTA 700 °C sample, which corresponds to the capacitance plateau of the GaAsN QW electron states signal. The emission times at high temperatures can be connected by a straight line from which emission energy is obtained, which increases from (a) 0.073 to 0.206 eV from  $-1.5$  to  $-4.4 \text{ V}$  for the as-grown sample and (b) 0.075 to 0.16 eV from  $-2.75$  to  $-4 \text{ V}$  for RTA 700 °C sample. Incidentally, the emission time of the GaAsN QW electron states after RTA at 800 °C for 3 min is too short to be obtained from C-F measurement. The emission times of the GaAsN QW electron states for the as-grown sample exhibit not only the thermal emission behavior ( $\tau T^2 \propto \exp(1/T)$ ) from  $-2.6$  to  $-4.4 \text{ V}$  but also a slight tunneling emission behavior ( $\tau$  is independent of  $1/T$ ) at low temperatures from  $-1.5$  to  $-1.9 \text{ V}$ . After thermal annealing, the bias range of the thermal emission behavior is decreased

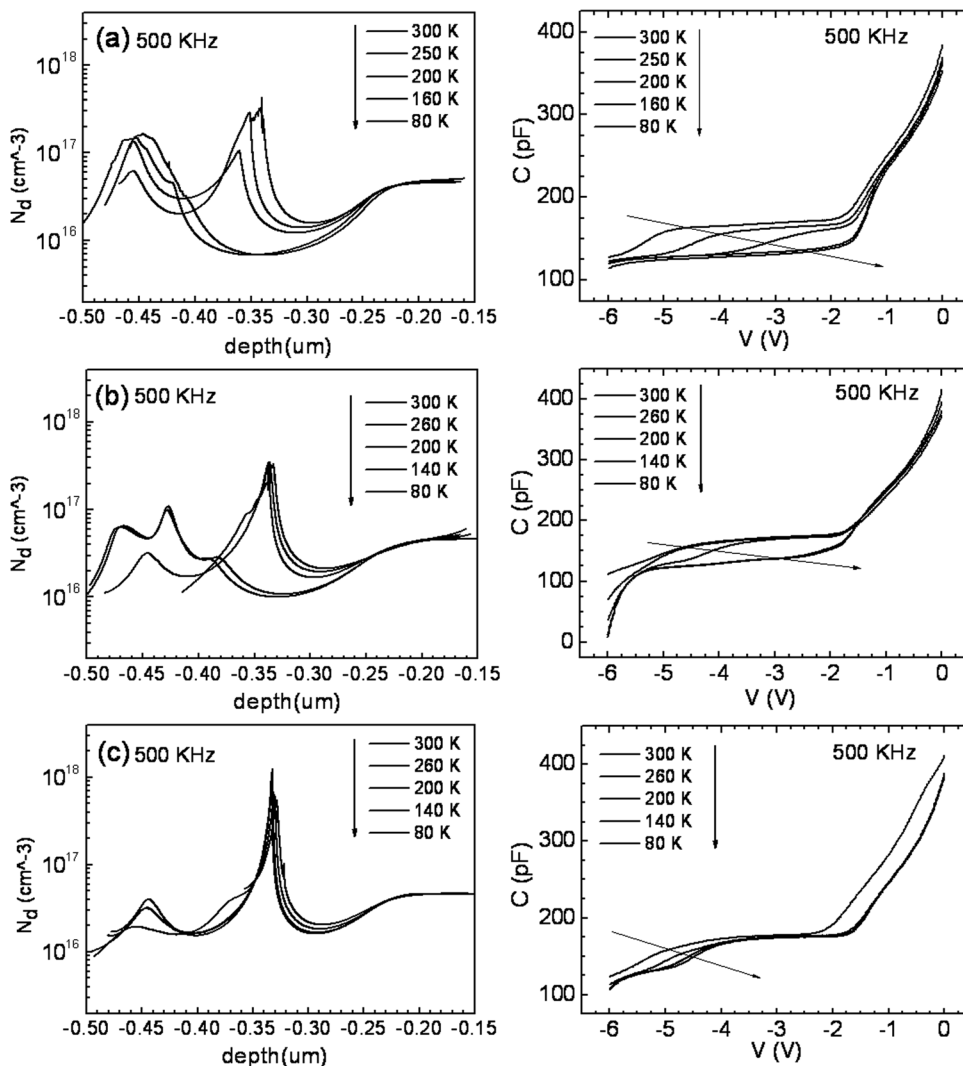


FIG. 2. 500 kHz temperature-dependent C-V depth profiles and the corresponding C-V spectra (as shown on the right side) of the 80 Å (a) as-grown, (b) RTA 700 °C, and (c) RTA 800 °C samples.

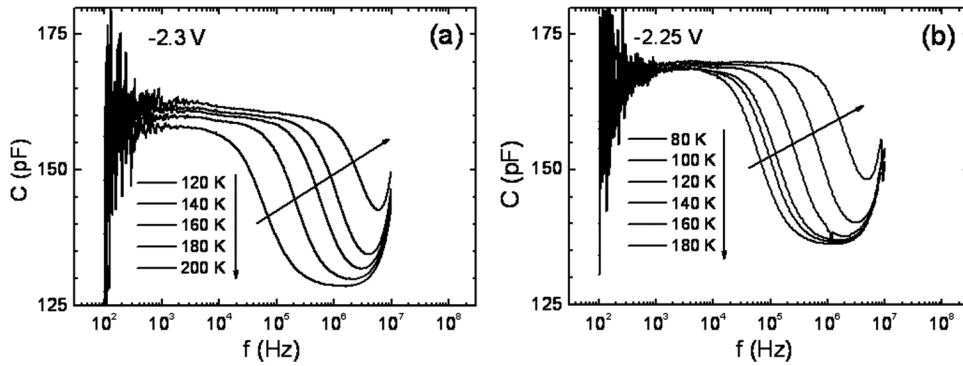


FIG. 3. Temperature-dependent C-F spectra measured at (a)  $-2.3$  V for as-grown sample and (b)  $-2.25$  V for RTA  $700^\circ\text{C}$  sample, corresponding to the frequency dispersion of the GaAsN QW electron states signal.

(from  $-3.25$  to  $-4$  V). Also, the tunneling emission behavior at low temperature occurs at the larger biases (from  $-1.5$  to  $-2.75$  V), indicating that the thermal annealing recovers the typical tunneling emission of a high-quality QW.

The correlation between QW electron emission behavior and thermal annealing is analyzed by using the phonon-assisted (field-assisted) tunneling model<sup>21</sup> combined with Schottky depletion theory.<sup>27</sup> According to this model, Fig. 5(a) summarizes the electron escape mechanism. Clearly, the QW electrons are not directly thermally activated into the GaAs barrier, since the confinement energy ( $E$ ) of electron ground state in our GaAsN QW is around  $0.347\sim 0.357$  eV below the GaAs barrier, according to the emission energy ( $E_{\text{GaAs}}$  ( $1.517$  eV) – GaAsN QW emission energy ( $1.16$  eV for the as-grown sample and  $1.17$  eV for RTA  $700^\circ\text{C}$  sample) at  $30$  K) obtained from PL measurements, under the assumption of negligible valence band offset.<sup>22–26</sup> Thus, the obtained activation energies suggest a two-step activation process: thermal activation to the GaAsN QW excited state and then subsequent tunneling into the GaAs, by the assistance of electric field. As mentioned earlier, severe N-composition fluctuation occurs in our GaAsN QW, leading to the broad PL linewidth of the GaAsN QW emission. The broad PL linewidth of the GaAsN QW emission indicates that the GaAsN QW electron states have a broad distribution. Hence, the GaAsN QW electron states are widely distributed

above the GaAsN CB. This finding indicates that the excited states for subsequent tunneling are widely distributed above the GaAsN CB, explaining why the phonon-assisted tunneling exhibits a continuum states behavior. Based on the Schottky depletion theory,<sup>27</sup> the applied bias represents the position of Fermi level. Therefore, the decrease of the applied bias shifts the Fermi level upward, leading to the observation of the upper excited states of GaAsN QW, as shown in Fig. 4. According to phonon-assisted tunneling model,<sup>21</sup> the total electron emission rate  $e_n$  (electron emission rate ( $e_n$ ) =  $1/\text{electron emission time } (\tau)$ ) for such thermally activated tunneling can then be determined by the product of the thermal emission rate ( $e_{\text{th}}$ ) and tunneling emission rate ( $e_{\text{tun}}$ ). The thermal emission rate can be written as

$$e_{\text{th}} = \gamma T^2 \sigma_{\infty} \exp\left(\frac{-E_a}{KT}\right),$$

where  $E_a$  is the activation energy,  $\sigma_{\infty}$  the capture cross section for  $T = \infty$ , and  $\gamma$  is a temperature-independent constant. In the phonon-assisted tunneling model, since carriers are emitted to the bottom GaAs electrode, the tunneling probability is related to the tunneling barrier height ( $E_b$ ) and the depletion width  $L$  (tunneling width) in bottom GaAs layer. Hence, under the assumption of a triangular barrier, the tunneling emission rate can be written as

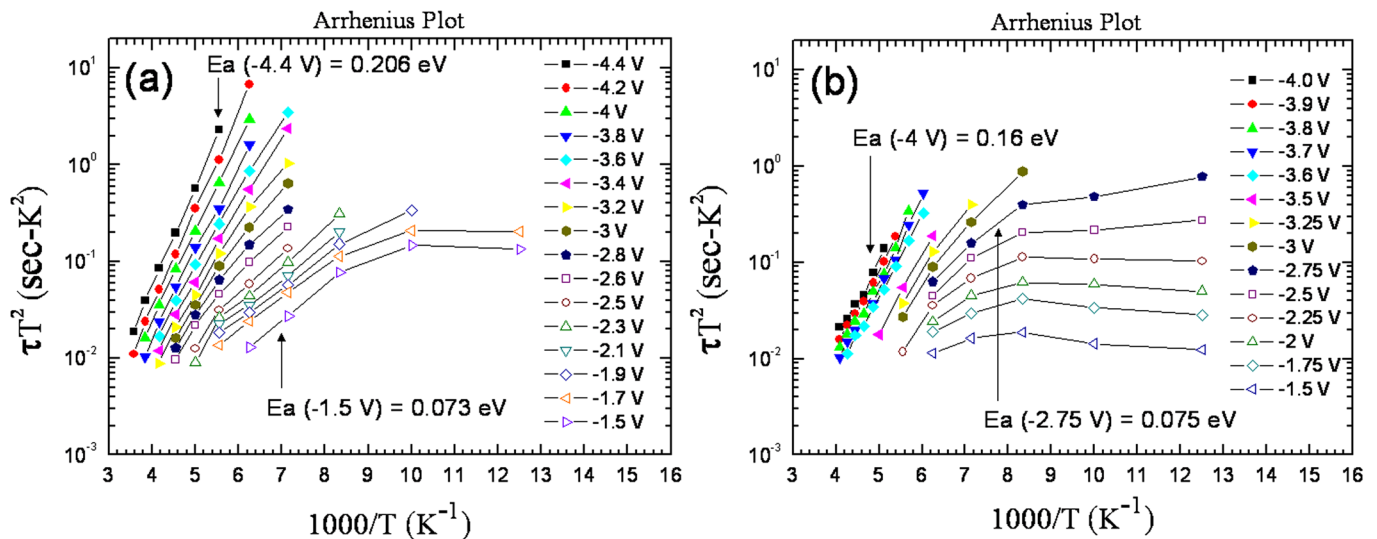


FIG. 4. (Color online) Arrhenius plots of the emission times of the GaAsN QW electron states, as obtained from the C-F spectra from (a)  $-1.5$  to  $-4.4$  V for as-grown sample and (b)  $-1.5$  V to  $-4$  V for RTA  $700^\circ\text{C}$  sample.

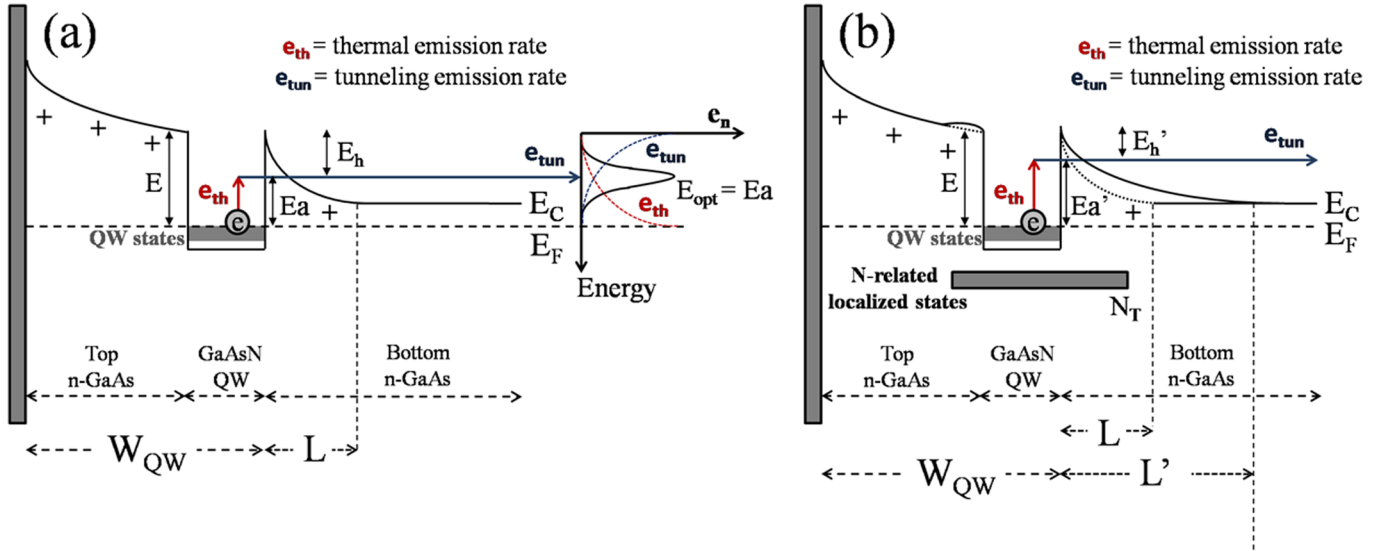


FIG. 5. (Color online) Schematic band diagram that illustrates the electron emission from the GaAsN QW electron states (a) without and (b) with the N-related localized states.

$$e_{\text{tun}} = \frac{eF}{4\sqrt{2m^*E_h}} \exp\left[-\frac{4\sqrt{2m^*}(E_h)^{3/2}}{3e\hbar F}\right],$$

where  $F$  is the electric field in depletion region of bottom GaAs,  $m^*$  is the GaAs effective mass,  $e$  is the electron charge, and  $E_h$  is the tunneling barrier height. Furthermore, the relation between the activation energy ( $E_a$ ) and the tunneling barrier height ( $E_h$ ) can be expressed as follows:  $E_a = E - E_h$ , as shown in Fig. 5(a). As schematically depicted in Fig. 5(a), both the thermal emission rate  $e_{\text{th}}$  and tunneling emission rate  $e_{\text{tun}}$  depend exponentially on energy but have opposing tendencies. This means that the total electron emission rate ( $e_n$ ) will reach a maximum at a certain optimal energy  $E_{\text{opt}}$ , depending on the electric field ( $F$ ) in depletion region of bottom GaAs. This optimal energy plays a decisive role in the electron escape process. The electron can find an available excited state near the optimal energy as an optimal intermediate state for the subsequent tunneling process. Therefore, the QW electron emission behavior is dependent on which process (thermal or tunneling) is predominant in the electron escape process. In a same QW electron state (fixed  $E$ ), as electric field in depletion region of bottom GaAs layer increasing (decreasing), the tunneling emission rate is larger (smaller) than the thermal emission rate, and thus the tunneling (thermal) emission process is predominant in the electron emission behavior. Besides, in a same QW electron state (fixed  $E$ ), as temperature decreasing (increasing), the thermal emission rate is thus decreased (increased), resulting in the electron emission behavior exhibiting a tunneling (thermal) emission behavior at low (high) temperature. This result is consistent with the observed QW electron emission behavior in Fig. 4, which exhibits tunneling emission behavior at low temperature, which is in contrast with the thermal emission behavior at high temperature. Therefore, the electric field ( $F$ ) in depletion region of bottom GaAs layer and temperature ( $T$ ) are closely associated with the QW electron emission

behavior. Furthermore, according to the Schottky depletion theory,<sup>27</sup> the electric field ( $F$ ) in depletion region of bottom GaAs layer and the confinement energy ( $E$ ) of the probed QW electrons can be written as

$$F = \frac{e}{\varepsilon}(N_D - N_T)L,$$

$$E = \frac{e}{2\varepsilon}(N_D - N_T)L^2 + \frac{KT}{e} \ln\left(\frac{N_C}{N_D}\right),$$

where  $\varepsilon$  is the permittivity of the semiconductor,  $e$  is the electron charge,  $N_D$  is the sample doping concentration,  $N_T$  is the trap concentration in the GaAs bottom layer,  $L$  is the depletion width of bottom GaAs layer, and  $N_C$  is the effective density of states in the GaAs CB. Therefore, in a same QW electron state (fixed  $E$ ), as trap concentration ( $N_T$ ) in bottom GaAs layer increasing, the depletion width of bottom GaAs layer ( $L$ ) also will be increased, which is consistent with the form

$$L \propto \frac{1}{\sqrt{N_D - N_T}}.$$

Substituting  $L$  into the formula of electric field ( $F$ ) yields the relation between  $F$  and  $N_T$  as

$$F \propto \sqrt{N_D - N_T}.$$

As mentioned earlier, the N-related localized states are attributed to the clusters of N atoms in the GaAsN QW. During the growth of the GaAsN QW, the N atoms are possible to diffuse into the neighboring GaAs layer (bottom and top). Thus, more than just located at the GaAsN QW region, the N-related localized states are also extended into the neighboring GaAs layer (bottom and top), as shown in Fig. 5(b). Figure 5 shows the schematic band diagram for illustrating the electron emission from the GaAsN QW electron states

(a) without and (b) with the N-related localized states. By comparing between Figs. 5(a) and 5(b), as the GaAsN QW with the N-related localized states ( $N_T$ ), the depletion width of bottom GaAs layer (L) is relatively large (from L to L'), and the electric field (F) in depletion region of bottom GaAs layer is relatively small. Consequently, the electrons in the GaAsN QW electron states must be thermally activated to the upper excited states and then tunnel into the bottom GaAs, ultimately leading to the electron emission behavior for the as-grown sample almost exhibiting a thermal emission behavior. Thus, the presence of N-related localized states effectively suppresses the tunneling emission behavior of the GaAsN QW electron states. Moreover, removing the N-related localized states ( $N_T$ ) can restore the depletion width of bottom GaAs layer (from L' to L), and the electric field (F) in depletion region of bottom GaAs layer is thus increased, resulting in a recovery of the tunneling emission behavior for GaAsN QW electron states.

Figure 6 shows the DLTS spectra of the 80 Å (a) as-grown, (b) RTA 700 °C, and (c) RTA 800 °C samples at the sweeping voltage ((a) -3 V/-3.5 V, (b) -3 V/-3.5 V, and (c) -3.5 V/-4 V). Based on the Schottky depletion theory,<sup>27</sup> the sweeping voltages of these DLTS measurements are correspond to the depletion region of bottom GaAs layer. According to this figure, all of these samples have an apparent peak at around 200 K~250 K; in addition, the as-grown sample has an additional peak at around 130~160 K. According to the above studies, in the as-grown sample, the emission time of the GaAsN QW electron states at 140 K under -3.6 V is about 0.2 ms, which is close to the time constant (0.43 ms at 140 K) of the additional peak at the sweeping voltage -3 V/-3.5 V obtained from DLTS measurement. Thus, the additional peak in Fig. 6(a) is attributed to the GaAsN QW electron states signal. Hence, the apparent peak at around 200 K~250 K originates from the electron trap states in the depletion region of bottom GaAs layer. Figure 7 shows the Arrhenius plots of the emission times of the electron trap states obtained from the DLTS spectra before annealing (square point) and after annealing at 700 °C (circle point), and 800 °C (triangle point). The activation energy (capture cross section) obtained from Fig. 7 is 0.424 eV ( $0.815 \times 10^{-13} \text{ cm}^2$ ) for the as-grown sample, 0.414 eV ( $4.123 \times 10^{-13} \text{ cm}^2$ ) for the RTA 700 °C sample, and 0.428 eV ( $1.347 \times 10^{-13} \text{ cm}^2$ ) for the RTA 800 °C sample. The activation energy corre-

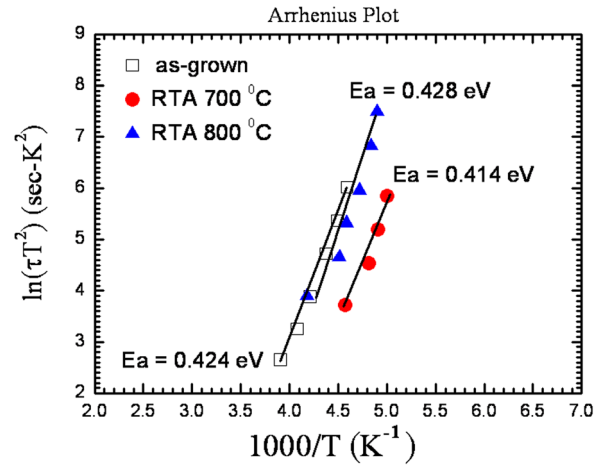


FIG. 7. (Color online) Arrhenius plots of the emission times of the electron trap states, as obtained from the DLTS spectra before annealing (square point) and after annealing at 700 °C (circle point), and 800 °C (triangle point).

sponds to the confinement energy of the electron trap states with respect to the GaAs CB. Thus, the electron trap states are located at about 0.414~0.428 eV below the GaAs CB. According to the PL measurement results, the emission energy of N-related localized states at 30 K is 1.15 eV for RTA 700 °C sample, and 1.17 eV for RTA 800 °C sample; the bandgap of GaAs at 30 K is about 1.517 eV. Therefore, the confinement energy of N-related localized states with respect to the GaAs CB can be obtained, under the assumption of negligible valence band offset.<sup>22-26</sup> Consequently, the N-related localized states are located at around  $0.347 \text{ (} 1.517 \text{ eV} - 1.17 \text{ eV)} \sim 0.367 \text{ eV}$  ( $1.517 \text{ eV} - 1.15 \text{ eV}$ ) below the GaAs CB. This finding is comparable to the activation energy of the electron trap states obtained from the DLTS measurement (0.414~0.428 eV) and also confirms that the electron trap states observed from the DLTS measurement originate from the electron emission of the N-related localized states. Thus, more than just optical electron trap states, the N-related localized states are also electrical electron trap states. Moreover, the trap concentration ( $N_T$ ) of the N-related localized states can be extracted from the DLTS measurement,<sup>27</sup> and the trap concentration is  $N_T = 5.8 \times 10^{14} \text{ cm}^{-3}$  for the as-grown sample,  $N_T = 3.6 \times 10^{14} \text{ cm}^{-3}$  for the RTA 700 °C sample, and  $N_T = 1.1 \times 10^{14} \text{ cm}^{-3}$  for the RTA 800 °C

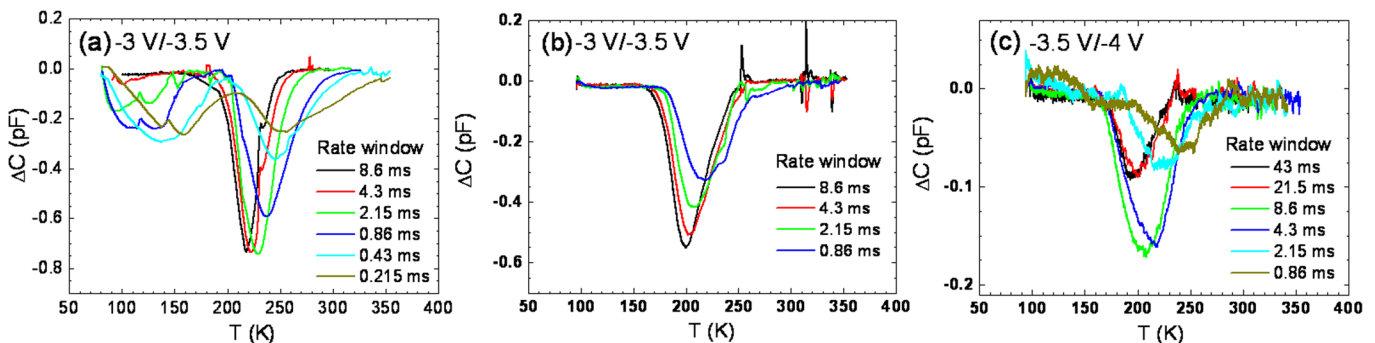


FIG. 6. (Color online) (a) DLTS spectra of the 80 Å as-grown sample, measured by sweeping the bias from -3 to -3.5 V. (b) DLTS spectra of the 80 Å RTA 700 °C sample, as measured by sweeping the bias from -3 to -3.5 V. (c) DLTS spectra of the 80 Å RTA 800 °C sample, measured by sweeping the bias from -3.5 to -4 V. The sweeping voltages of these DLTS measurements are correspond to the depletion region of bottom GaAs layer.

sample. Thus, our as-grown sample contains a considerable amount of N-related localized states, which can be reduced via thermal annealing. Increasing the annealing temperature can further reduce the number of N-related localized states in GaAsN QW. Consequently, the long electron emission time constant for the GaAsN QW electron states is due to the considerable number of N-related localized states in our as-grown sample. Thermal annealing can reduce the number of N-related localized states, resulting in a recovery of the tunneling emission for GaAsN QW electron states. Additionally, increasing the annealing temperature can significantly decrease the emission times of the GaAsN QW electron states, and restore the electron emission behavior of GaAsN QW to the typical electron tunneling emission for a high-quality QW. Incidentally, the confinement energies of N-related localized states were obtained by the DLTS spectra at around 200 K ~ 250 K because the DLTS system probe times constants around ms. To compare with the DLTS measurement results for obtaining the confinement energy of N-related localized states, we need to modify PL transition energy of N-related localized states to around 200 K ~ 250 K. However, the luminescence efficiency of GaAsN QW and N-related localized states emissions is deteriorated at high temperature (above 120 K) due to the lack of hole confinement in the QW. In the GaAs/GaAsN system, the band gap bowing is commonly accepted to be mainly in the CB with a very small VB offset. Hence, the confinement energy of holes in the QW is very small, resulting in the lack of hole confinement at high temperature. In addition, the PL emission of N-related localized states is difficult to identify separately after 90 K. Thus, we cannot directly observe the PL transition energy of N-related localized states at around 200 K ~ 250 K. Nevertheless, we still attempt to discuss the influence of temperature difference. To do this, we have measured the temperature-dependence PL transition energy of N-related localized states for RTA 800 °C sample (not shown here), and an extremely small decrease of 9 meV for PL transition energy of N-related localized states from 30 to 90 K. Next, we use the assumption of a linear decrease in the PL transition energy for N-related localized states during increasing temperature. For linear assumption ( $\frac{-9 \text{ meV}}{90 \text{ K} - 30 \text{ K}} = -0.15 \frac{\text{meV}}{\text{K}}$ ), we assume that the decrease of PL transition energy of N-related localized states from 30 to 200 K is less than 26 meV. Hence, the comparison of the confinement energies of N-related localized states between the DLTS measurement results and the PL measurement results is reasonable, since the influence of temperature difference between these measurements is less significant in our analysis.

To further provide the evidence about the influence of N-related localized states on the electron emission properties of quantum well. We use InGaAsN SQW samples with different growth rates to support our conclusion that the existence of N-related localized states can effectively suppress the tunneling emission of QW electron states. The In incorporation in this material system can assist us to obtain high-quality QW. Therefore, the InGaAsN SQW samples are suitable to verify the role of the N-related localized states in the electron emission properties of quantum well. Figure 8 shows the PL spectra (at 30 K) and the corresponding

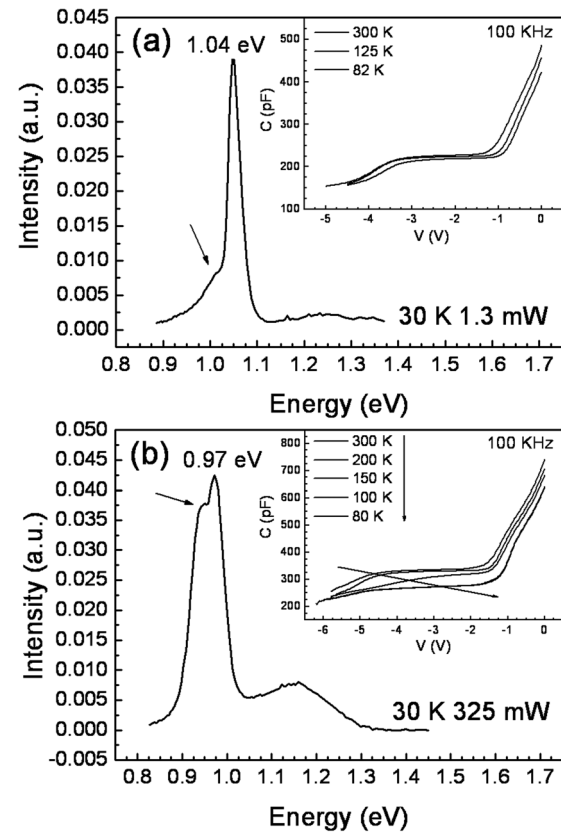


FIG. 8. 30 K PL spectra and the corresponding temperature-dependent C-V spectra at 100 kHz (in the inset) for the InGaAsN layers deposited at (a) 4.4 A/s (NGR) and (b) 2.8 A/s (LGR), respectively.

temperature-dependent C-V spectra at 100 kHz (in the inset) for the InGaAsN layers deposited at (a) 4.4 A/s (NGR) and (b) 2.8 A/s (LGR), respectively. In Fig. 8(a), the main peak at 1.04 eV is InGaAsN QW emission peak, and the low-energy tail (indicated by an arrow) is attributed to the N-related localized states induced by N-composition fluctuation. In an InGaAsN layer grown at a normal growth rate, the quality of InGaAsN QW is superior. Hence, only a slight inevitable N-composition fluctuation arises in the normal growth rate sample, resulting in only a few amounts of N-related localized states in this sample. Consequently, the emission peak of N-related localized states emerges as a low-energy tail at the left side of InGaAsN QW emission peak. According to our conclusion, in this study, since only a few amounts of N-related localized states in this sample, the electron emission behavior of InGaAsN QW is must be the typical electron tunneling emission, thus exhibiting a short electron emission time constant. Therefore, even at low temperature, the electron emission from InGaAsN QW electron states can follow the high-frequency ac signal, as shown in the inset of Fig. 8(a). These results can be correspond to the electron emission behavior of GaAsN QW after annealing at 800 °C, which exhibits a typical electron tunneling emission for a high-quality QW. In Fig. 8(b), lowering the growth rate to 2.8 A/s causes a slight redshift of the InGaAsN QW emission peak (to 0.97 eV) presumably due to an increased N content since only In and Ga fluxes are scaled down and also enhances the low-energy tail which becomes a pronounced



shoulder (indicated by an arrow) with comparable intensity as the InGaAsN QW emission. Lowering the growth rate of InGaAsN layer, the N atoms have enough time to segregate and cluster in the InGaAsN layer, leading to the degradation of the N-composition fluctuation and the drastic clustering of the N atoms. Therefore, the low growth rate sample has extensive N-related localized states, resulting in the raise of the emission peak of N-related localized states. Similarly, as discussed in this study, the N-related localized states effectively suppress the tunneling emission of the QW electron states, leading to a long electron emission time constant for the QW electron states. Thus, the electron emission from InGaAsN QW electron states cannot follow the high-frequency ac signal at low temperature, as shown in the inset of Fig. 8(b). These results also can be correspond to the electron emission behavior of our as-grown GaAsN QW sample, which exhibits a long electron emission time constant. Therefore, based on the above results, the presence of N-related localized states in QW certainly suppresses the tunneling emission of QW electron states, leading to a long electron emission time for the QW electron states.

#### IV. CONCLUSIONS

This study elucidates the influence of the N-related localized states on electron emission properties of a GaAsN QW. The N-related localized states are identified by optical and electrical measurements. Thus, more than just optical electron trap states, the N-related localized states in GaAsN quantum well are also electrical electron trap states. Furthermore, exactly how N-related localized states influence electron emission properties of GaAsN quantum well is investigated based on experimental results and a theoretical model. According to those results, the N-related localized states effectively suppress the tunneling emission of the GaAsN QW electron states, leading to a long electron emission time constant for the GaAsN QW electron states. Thermal annealing can reduce the number of N-related localized states, resulting in a recovery of the tunneling emission for GaAsN QW electron states. Increasing the annealing temperature can significantly decrease the emission times of the GaAsN QW electron states, as well as restore the electron emission behavior of GaAsN QW to the typical electron tunneling emission for a high-quality QW.

#### ACKNOWLEDGMENTS

The authors would like to thank the National Science Council of the Republic of China, Taiwan, for financially supporting this research under Contract No. NSC-97-2112-M-009-014-MY3, as well as the MOE ATU program for its support.

- <sup>1</sup>M. C. Larson, M. Kondow, T. Kitatani, K. Nakahara, K. Tamura, H. Inoue, and K. Uomi, *IEEE Photonics Technol. Lett.* **10**, 188 (1998).
- <sup>2</sup>J. S. Harris, Jr., *Semicond. Sci. Technol.* **17**, 880 (2002).
- <sup>3</sup>M. Bosi and C. Pelosi, *Prog. Photovoltaics* **15**, 51 (2006).
- <sup>4</sup>M. Henini, *Dilute Nitride Semiconductors* (Elsevier, Oxford, 2005), Chap. 4.
- <sup>5</sup>I. A. Buyanova, W. M. Chen, G. Pozina, J. P. Bergman, B. Monemar, H. P. Xin, and C. W. Tu, *Appl. Phys. Lett.* **75**, 501 (1999).
- <sup>6</sup>R. Kudrawiec, G. Sek, J. Misiewicz, L. H. Li, and J. C. Harmand, *Eur. Phys. J.: Appl. Phys.* **27**, 313 (2004).
- <sup>7</sup>P. R. C. Kent and A. Zunger, *Phys. Rev. Lett.* **86**, 2613 (2001).
- <sup>8</sup>P. R. C. Kent and A. Zunger, *Phys. Rev. B* **64**, 115208 (2001).
- <sup>9</sup>J. F. Chen, C. T. Ke, P. C. Hsieh, C. H. Chiang, W. I. Lee, and S. C. Lee, *J. Appl. Phys.* **101**, 123515 (2007).
- <sup>10</sup>H. Kalt and M. Hetterich, *Optics of Semiconductors and Their Nanostructure* (Springer, Berlin, 2004).
- <sup>11</sup>W. K. Cheah, W. J. Fan, S. F. Yoon, W. K. Loke, R. Liu, and A. T. S. Wee, *J. Appl. Phys.* **99**, 104908 (2006).
- <sup>12</sup>C. Skierbiszewski, S. P. Lepkowski, P. Perlin, T. Suski, W. Jantsch, and J. Geisz, *Physica E* **13**, 1078 (2002).
- <sup>13</sup>M.-A. Pinault and E. Tournie, *Appl. Phys. Lett.* **79**, 3404 (2001).
- <sup>14</sup>E. V. K. Rao, A. Ougazzaden, Y. Le Bellego, and M. Juhel, *Appl. Phys. Lett.* **72**, 1409 (1998).
- <sup>15</sup>S. Francoeur, G. Sivaraman, Y. Qiu, S. Nikishin, and H. Temkin, *Appl. Phys. Lett.* **72**, 1857 (1998).
- <sup>16</sup>L. H. Li, Z. Pan, W. Zhang, Y. W. Lin, Z. Q. Zhou, and R. H. Wu, *J. Appl. Phys.* **87**, 245 (2000).
- <sup>17</sup>D. Kwon, R. J. Kaplar, S. A. Ringel, A. A. Allerman, S. R. Kurtz, and E. D. Jones, *Appl. Phys. Lett.* **74**, 2830 (1999).
- <sup>18</sup>R. Kudrawiec, G. Sek, J. Misiewicz, F. Ishikawa, A. Trampert, and K. H. Ploog, *Appl. Phys. Lett.* **94**, 011907 (2009).
- <sup>19</sup>I. A. Buyanova, W. M. Chen, B. Monemar, H. P. Xin, and C. W. Tu, *Mater. Sci. Eng., B* **75**, 166 (2000).
- <sup>20</sup>X. D. Luo, Z. Y. Xu, W. K. Ge, Z. Pan, L. H. Li, and Y. W. Liu, *Appl. Phys. Lett.* **79**, 958 (2001).
- <sup>21</sup>G. Vincent, A. Chantre, and D. Bois, *J. Appl. Phys.* **50**, 5484 (1979).
- <sup>22</sup>A. Grau, T. Passow, and M. Hetterich, *Appl. Phys. Lett.* **89**, 202105 (2006).
- <sup>23</sup>W. Shan, W. Walukiewicz, K. M. Yu, J. W. Ager III, E. E. Haller, J. F. Geisz, D. J. Friedmann, J. M. Olson, S. R. Kurtz, H. P. Xin, and C. W. Tu, *Phys. Status Solidi B* **223**, 75 (2001).
- <sup>24</sup>L. Bellaiche and A. Zunger, *Phys. Rev. B* **57**, 4425 (1998).
- <sup>25</sup>S. H. Wei and A. Zunger, *Phys. Rev. Lett.* **76**, 664 (1996).
- <sup>26</sup>W. G. Bi and C. W. Tu, *Appl. Phys. Lett.* **70**, 1608 (1997).
- <sup>27</sup>D. K. Schroder, *Semiconductor Material and Device Characterization* (Wiley, New York, 2006).